Inorganic Chemistry
Article
pubs.acs.org/IC

Synthesis and Characterization of 12-Pyridinium Derivatives of the [*closo*-1-$CB_{11}H_{12}$]$^-$ Anion

Jacek Pecyna,[†] Bryan Ringstrand,[†] Sławomir Domagała,[‡] Piotr Kaszyński,*[,†,§] and Krzysztof Woźniak[‡]

[†]Organic Materials Research Group, Department of Chemistry, Vanderbilt University, Nashville, Tennessee 37235, United States
[‡]Department of Chemistry, University of Warsaw, 02-089 Warsaw, Poland
[§]Faculty of Chemistry, University of Łódź, 91403 Łódź, Poland

Supporting Information

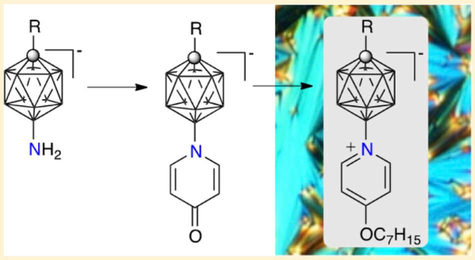

ABSTRACT: Diazotization of [*closo*-1-$CB_{11}H_{10}$-1-R-12-NH_2]$^-$[NMe_4]$^+$ (**4[NMe$_4$]**) in neat 4-methoxypyridine leads to 12-(4-methoxypyridinium) zwitterions [*closo*-1-$CB_{11}H_{10}$-1-R-12-(4-$MeOC_5H_4N$)] (**2**) in ~50% yield. Demethylation of **2** with LiCl in dimethylformamide provides access to 12-pyridones **5[NMe$_4$]**, which can be O-alkylated with alkyl triflates giving 12-(4-alkoxypyridinium) zwitterions, such as **1**. This three-step process is more efficient than direct diazotization of amine **4[NMe$_4$]** in neat higher 4-alkoxypyridine. The new method was demonstrated for the synthesis of [*closo*-1-$CB_{11}H_{10}$-1-C_5H_{11}-12-(4-$C_7H_{15}OC_5H_4N$)] (**1c**), which exhibits a smectic A phase. Molecular and electronic structures of 4-methoxypyridinium zwitterion **2b** and its C(1) isomer [*closo*-1-$CB_{11}H_{11}$-1-(4-$MeOC_5H_4N$)] (**3b**) were investigated by single-crystal X-ray diffraction and spectroscopic methods, respectively, and the experimental results were compared to those obtained with density functional theory methods. Lastly, the mechanism for formation of zwitterions **2** was investigated computationally revealing low energy for dediazoniation of the [*closo*-1-$CB_{11}H_{10}$-1-R-12-N_2] (**14**) intermediate ($\Delta G_{298} \approx 25$ kcal/mol) to form boronium ylide **15**, with weak dependence on substituent R. Dinitrogen derivative **14c** was observed by ^{11}B NMR spectroscopy.

INTRODUCTION

Zwitterionic derivatives **I** and **II** of monocarbaborates [*closo*-1-CB_9H_{10}]$^-$ (**A**) and [*closo*-1-$CB_{11}H_{12}$]$^-$ (**B**, Figure 1) possess large longitudinal dipole moments and for this reason are of interest as core elements of polar liquid crystals[1] suitable for electro-optical applications.[2] In this context, we initially investigated 1-sulfonium derivatives of type **IA**,[3,4] and later we developed a convenient method for access to 1-pyridinium zwitterions of anions **A** and **B**.[5] Although materials of type **IA** and **IB** are effective additives that increase dielectric anisotropy $\Delta\varepsilon$ of a nematic liquid crystal host, these polar materials rarely exhibit liquid crystalline properties themselves, have high melting points, and display limited solubility in nematic hosts.

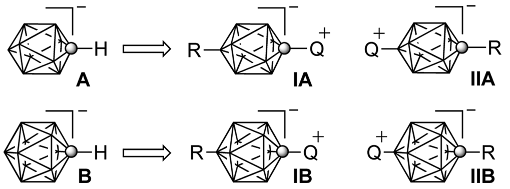

Figure 1. Structures of the [*closo*-1-CB_9H_{10}]$^-$ and [*closo*-1-$CB_{11}H_{12}$]$^-$ anions (**A** and **B**) and their zwitterionic 1,10- (**IA**, **IIA**) and 1,12-disubstituted (**IB**, **IIB**) derivatives. Q^+ represents an onium fragment such as quinuclidinium, sulfonium, or pyridinium. Each vertex represents a BH fragment, and the sphere is a carbon atom.

We sought to improve the properties of materials derived from monocarbaborates **A** and **B** by focusing on structures **IIA** and **IIB**, in which the onium fragment is attached to the B(10) and B(12) positions of the anions, respectively. Pyridinium and sulfonium zwitterions **IIA**, prepared from relatively stable 10-dinitrogen derivatives of the [*closo*-1-CB_9H_{10}]$^-$ anion (**A**), showed great promise. These compounds have lower melting points, often form nematic phases, and display greater solubility in nematic hosts relative to structures of type **I**, while maintaining a sizable longitudinal dipole moment and high $\Delta\varepsilon$ values.[4,6] Although the chemistry of the [*closo*-1-CB_9H_{10}]$^-$ anion (**A**) is well-understood and straightforward,[7] the [*closo*-1-$CB_{11}H_{12}$]$^-$ anion[8] (**B**) is more accessible[9,10] and, for this reason, is more attractive as a structural element of molecular materials. Functionalization of the former anion and preparation of zwitterionic materials is conveniently achieved through dinitrogen derivatives as the key intermediates.[11−13] Unfortunately, analogous dinitrogen derivatives of the [*closo*-1-$CB_{11}H_{12}$]$^-$ anion (**B**) are generally much less stable, and their isolation appears impractical. This limitation significantly reduces access to zwitterionic derivatives of the [*closo*-1-$CB_{11}H_{12}$]$^-$ anion (**B**). Nonetheless, we recently demonstrated that even unstable dinitrogen derivatives of monocarbaborates, such as [*closo*-1-CB_9H_8-1-COOH-6-N_2],[14] can be synthetically useful, when formed *in situ* as transient species during

Received: September 19, 2014
Published: November 13, 2014

diazotization of the corresponding amines. For example, diazotization of [*closo*-1-$CB_{11}H_{10}$-1-COOH-12-NH_3] in neat 4-heptyloxypyridine gave 6% yield of the desired pyridinium acid [*closo*-1-$CB_{11}H_{10}$-1-COOH-12-(4-$C_7H_{15}OC_5H_4N$)] (**1a**, Figure 2).[15] Since esters of **1a** and other compounds containing the pyridinium zwitterion are of interest as high $\Delta\varepsilon$ additives to liquid crystals, we set out to develop an alternative and more efficient method for the preparation of such compounds.

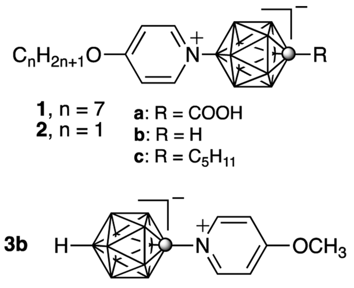

Figure 2. Structures of pyridinium zwitterions.

Here we report a simple and efficient method for the preparation of [*closo*-1-$CB_{11}H_{11}$-12-(4-$C_7H_{15}OC_5H_4N$)] (**1b**) and extend it to the preparation of liquid crystalline [*closo*-1-$CB_{11}H_{10}$-1-C_5H_{11}-12-(4-$C_7H_{15}OC_5H_4N$)] (**1c**) as a representative of a potentially diverse class of 12-(4-alkoxypyridinium) zwitterionic derivatives of [*closo*-1-$CB_{11}H_{12}$]$^-$ anion (**B**). The synthetic work is accompanied by mechanistic consideration augmented with density functional theory (DFT) computational results. We also take advantage of the available **2b** and compare its electronic and molecular structures with its C(1) isomer **3b** using experimental and computational methods.

RESULTS AND DISCUSSION

Synthesis. Diazotization of amine [*closo*-1-$CB_{11}H_{11}$-12-NH_2]$^-$[NMe_4]$^+$ (**4b[NMe$_4$]**) with [NO]$^+$[PF_6]$^-$ in neat 4-methoxypyridine at −20 °C, according to a general procedure,[14] gave 4-methoxypyridinium derivative **2b** in ~50% yield (Scheme 1). In contrast, diazotization of **4b[NMe$_4$]** in neat 4-heptyloxypyridine gave zwitterion **1b** in only 15% yield, which is over 3 times lower than that for **2b** and consistent with the 6% yield obtained for acid **1a** under the same conditions.[15]

Scheme 1. Synthesis of 4-Heptyloxypyridinium Derivatives 1[a]

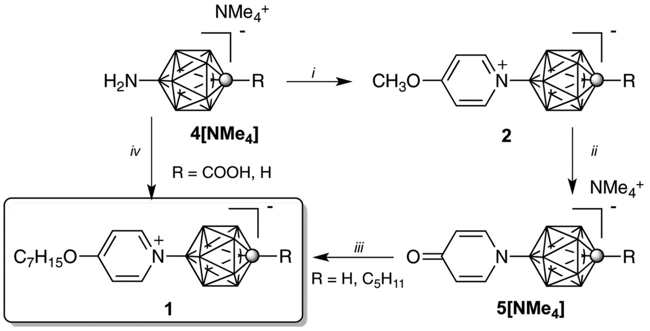

[a]Reagents and conditions: (*i*) 4-methoxypyridine, [NO]$^+$[PF_6]$^-$, −20 °C, 2 h; (*ii*) 1. LiCl, DMF, 80 °C; 2. [NMe_4]$^+$Cl$^-$; (*iii*) ROTf, CH_2Cl_2, rt; (*iv*) 4-heptyloxypyridine, [NO]$^+$[PF_6]$^-$, −20 °C, 2 h.

To increase the yield of 4-alkoxypyridinium zwitterions with longer or more diverse alkyl chains, another route to **1b** was explored starting from 4-methoxypyridinium derivative **2b**. Thus, the methyl group in **2b** was removed using LiCl in dimethylformamide (DMF)[16] giving pyridone **5b[NMe$_4$]** in quantitative yield. Subsequent O-alkylation of **5b[NMe$_4$]** with heptyl triflate[5] gave **1b** in 80% yield (Scheme 1) or 40% overall yield from amine **4b[NMe$_4$]**, which represents a significant improvement over the single-step procedure.

The requisite amine **4b[NMe$_4$]** was obtained in ~50% yield by Pd-catalyzed amination[12,17] of iodo derivative [*closo*-1-$CB_{11}H_{11}$-12-I]$^-$Cs$^+$ (**6b[Cs]**), which was prepared by iodination[18] of [*closo*-1-$CB_{11}H_{12}$]$^-$ anion (**B**) with I_2 in AcOH (Scheme 2). The iodination reaction leads, however, to a mixture of two regioisomers, namely, the 12- and 7-iodo derivatives **6b** and **7b**, respectively, in ~3:1 ratio. The desired pure 12-iodo isomer, [*closo*-1-$CB_{11}H_{11}$-12-I]$^-$ (**6b**), can be obtained by repeated recrystallization of its Cs$^+$ salt, **6b[Cs]**, from hot water. This is accomplished, however, with low mass recovery (typically less than 50%) and has significant impact on the overall yield of **1**. Therefore, higher efficiency of preparation of **1** could be achieved by improving the separation of isomers that are formed on early stages of the synthetic sequence.

To avoid losses of the desired **6b** the ionic isomers were carried forward without separation. Therefore, the sequence of amination and diazotization was performed on a 3:1 mixture of isomers **6b** and **7b**. Thus, amination of the mixture with LiHMDS in tetrahydrofuran (THF) gave a 3:1 mixture of amines **4b[NMe$_4$]** and [*closo*-1-$CB_{11}H_{11}$-7-NH_2]$^-$[NMe_4]$^+$ (**8b[NMe$_4$]**), which was diazotized in 4-methoxypyridine giving a mixture of 12-(4-methoxypyridinium) and 7-(4-methoxypyridinium) isomers, **2b** and **9b**, respectively (Scheme 2). The desired **2b** was easily and quantitatively separated from the more polar 7-isomer [*closo*-1-$CB_{11}H_{11}$-7-(4-$MeOC_5H_4N$)] (**9b**) by column chromatography.

The two protocols were used in tandem for the preparation of the 1-pentyl derivative **1c** from the parent anion [*closo*-1-$CB_{11}H_{12}$]$^-$ (**B**). Thus, following a general literature procedure,[18] the Cs$^+$ salt of anion **B** was treated with *n*-BuLi in the presence of tetramethylethylenediamine (TMEDA) and subsequently with 1-iodopentane to afford [*closo*-1-$CB_{11}H_{11}$-1-C_5H_{11}]$^-$Cs$^+$ (**10c[Cs]**) in 85% yield (Scheme 3). Iodination of **10c[Cs]** with I_2 in AcOH gave a mixture of isomers **6c** and **7c** in 77% yield, which upon amination with LiHMDS provided a mixture of isomers **4c[NMe$_4$]** and **8c[NMe$_4$]** in 81% yield (Scheme 2). Subsequent diazotization of the amines gave a mixture of the pyridinium derivatives **2c** and **9c**, out of which the desired [*closo*-1-$CB_{11}H_{10}$-1-C_5H_{11}-12-(4-$MeOC_5H_4N$)] (**2c**) was isolated in 45% yield. Thus, the overall yield for the synthesis is 12% based on anion **B**. No enrichment of a particular isomer was observed in this sequence of reactions.

Removal of the methyl group in **2c** gave pyridone [*closo*-1-$CB_{11}H_{10}$-1-C_5H_{11}-12-(4-OC_5H_4N)]$^-$[NMe_4]$^+$ (**5c[NMe$_4$]**), which upon treatment with heptyl triflate[5] yielded **1c** in nearly quantitative yield for the two-step process (Scheme 1).

Finally, for comparison purposes, 4-methoxypyridinium derivative **3b** was conveniently obtained by reacting 4-methoxypyrylium triflate (**11**) with amine [*closo*-1-$CB_{11}H_{11}$-1-NH_2]$^-$[NMe_4]$^+$ (**12[NMe$_4$]**) in 16% yield, according to a previously reported method (Scheme 4).[5] During recrystallization of **3b** from EtOH/H_2O, partial exchange of the methyl group for ethyl was observed. This suggests that the C(1) 4-methoxypyridinium derivative is also susceptible to demethy-

Scheme 2. Synthesis of 12-Pyridinium Derivatives[a]

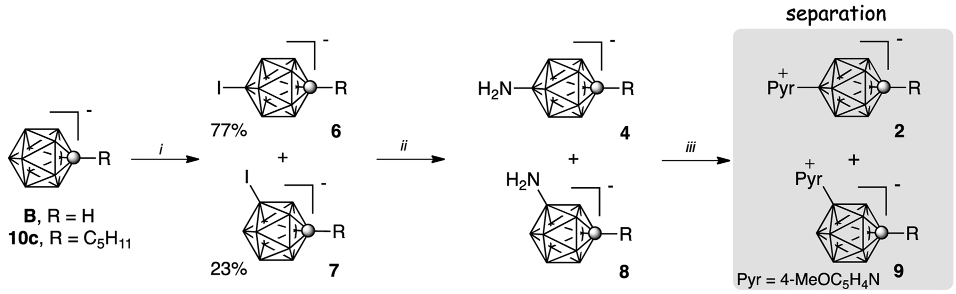

[a]Reagents and conditions: (*i*) I_2, AcOH, 50 °C, 72 h; (*ii*) Pd_2dba_3, 2-(Chx_2P)biphenyl, LiHMDS, THF, reflux, 72 h; (*iii*) 4-methoxypyridine, $[NO]^+[PF_6]^-$, −20 °C, 2 h.

Scheme 3. Synthesis of Pentyl Derivative 10c[Cs][a]

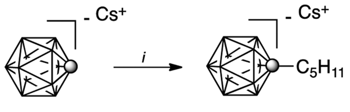

B[Cs] **10c[Cs]**

[a]Reagents and conditions: (*i*) 1. *n*-BuLi, TMEDA, THF, −78 °C; 2. *n*-$C_5H_{11}I$, 0 °C → rt.

Scheme 4. Preparation of 4-Methoxypyridinium Derivative 3b[a]

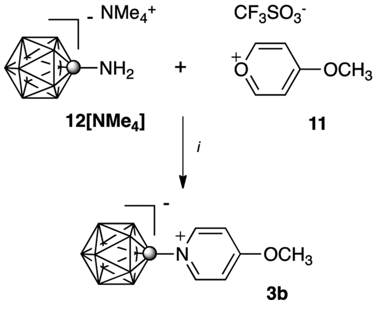

[a]Reagents and conditions: (*i*) THF, rt, 12 h.

lation and may provide means to more efficient preparation of higher C(1) 4-alkoxypyridinium homologues. These reactions were not pursued at this time.

Thermal Properties. Differential scanning calorimetry (DSC, Figure 3) and polarizing optical microscopy (POM, Figure 4) revealed that **1c** exhibits crystal polymorphism and an enantiotropic smectic A (SmA) phase between 111 and 143 °C.

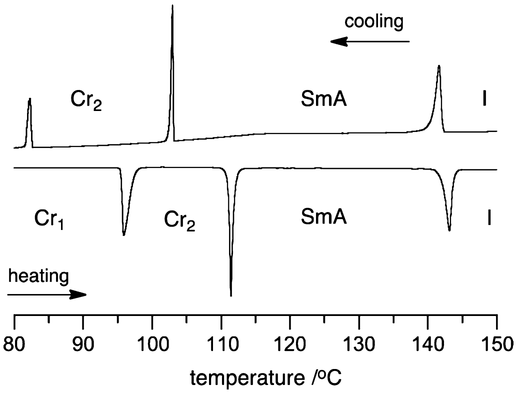

Figure 3. A DSC trace of **1c**. Cr - crystal; SmA - smectic A; I - isotropic. The heating and cooling rates are 5 K min^{-1}.

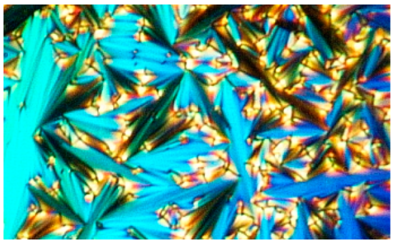

Figure 4. Optical texture of a SmA phase observed for **1c** at 130 °C on cooling from the isotropic phase.

This is in contrast to its constitutional isomer **13**:[5] exchanging positions of the substituents on the $\{1\text{-}CB_{11}\}$ cluster in **1c** leads to a substantial increase of the melting point and elimination of liquid crystalline properties (Figure 5). However, extension of the pentyl chain in **13** to decyl results in induction of an SmA phase with the isotropic transition at 200 °C.[5] The difference in thermal behavior of the two isomers is related to the stability of the crystalline phase governed by the magnitude of the molecular dipole moment: μ = 12.2 D for **1c** and μ = 18.2 D for **13**, according to B3LYP/6-31G(d,p) calculations in vacuum.

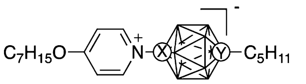

1c, X = B, Y = C: Cr_1 96 (*5.0*) Cr_2 111 (*5.4*) SmA 143 (*4.5*) I
13, X = C, Y = B: Cr 205 (*26.6*) I

Figure 5. A comparison of thermal properties for two isomers **1c** and **13**. Data for **13** was taken from ref 5.

Comparative Analysis of Isomers 2b and 3b. To gain a better understanding of the effect of substitution position of the pyridine ring on electronic and molecular structures of the zwitterions, two isomers, the 12-(4-methoxypyridinium) and 1-(4-methoxypyridinium) derivatives **2b** and **3b**, respectively, were investigated in detail.

Electronic Structures. Natural bond orbital (NBO) population analysis of the B3LYP/6-31G(d,p) wave function demonstrates differences in electron density distribution in both isomers, mainly at the ring−cage connection (Table 1). Thus, substitution of the pyridine for H atom on the cage results in depletion of electron density by ~0.3 e at the substituted atom, either B(12) or C(1). In **2b** the nitrogen

Table 1. Selected Electronic Parameters for 2b and 3b

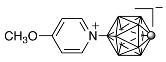

2b

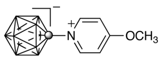

3b

	2b	3b
$q_{C(1)}$[a]	−0.71	−0.36
$q_{B(12)}$[a]	+0.17	−0.14
q_N[a]	−0.44	−0.28
q_{Me}[a]	−0.337	−0.338
μ/D[b]	11.6	16.7
rel ΔH/kcal mol^{-1}	0.0	+42.7
δ ($H_{2,6}$)/ppm[c]	8.47	8.83
δ ($H_{3,5}$)/ppm[c]	7.18	7.24
δ (Me)/ppm	4.01[c] (58.4)[d]	4.10[c] (59.4)[d]

[a] Atomic charge from the NBO analysis of the B3LYP/6-31G(d,p) wave function. [b] Dipole moment in vacuum. [c] ^{1}H NMR chemical shift of the pyridine fragment (CD_3CN). [d] ^{13}C NMR chemical shift (CD_3CN).

atom connected to the boron atom has higher electron density (−0.44 e) than in the **3b** isomer (−0.28e), which is connected to the carbon atom. This results in different polarization of the B−N bond and leads to significant differences in the calculated molecular dipole moment and thermodynamic stability of the two isomers: substitution of the pyridine fragment on the C(1) atom of the cluster increases the dipole moment by about 50% to 16.7 D and decreases stability by nearly 43 kcal mol^{-1} in vacuum (Table 1). Electron density of the MeO group is essentially the same in both isomers.

The difference in electron distribution in the two isomers affects the chemical shifts in NMR spectroscopy, and the "organic" H atoms in **2b** are generally more shielded relative to those in **3b**. For instance, hydrogen atoms in positions two and six of the pyridine ring are more shielded in the B(12) isomer by 0.36 ppm than they are in the C(1) isomer **3b** (Table 1). Similarly, the distant Me group is more shielded in **2b**, although the effect is appropriately weaker.

Electronic Absorption Spectroscopy. Both isomers **2b** and **3b** exhibit a single absorption band in the UV region with maximum ~250 nm (log $\varepsilon \approx 4.3$) in MeCN (Figure 6). The maximum for the C(1) isomer (**3b**) is shifted to lower energies by 9.5 nm or 187 meV relative to the B(12) derivative **2b**. Time-dependent (TD) DFT computational analysis of both compounds in MeCN dielectric medium reproduced well the experimental spectra. The electronic excitation energy for **2b** is calculated at 239 nm (f = 0.40) and involves mainly the HOMO, localized on the cluster, to the LUMO, localized on the pyridine fragment, transition (Figure 7). Similar TD-DFT analysis for the C(1)-pyridinium isomer **3b** demonstrated that the absorption band at 257 nm is composed of two transitions at 245 nm (HOMO → LUMO, f = 0.27) and 231 nm (HOMO−4 → LUMO, f = 0.20) both involving the {1-CB_{11}}-to-pyridine excitation.[10]

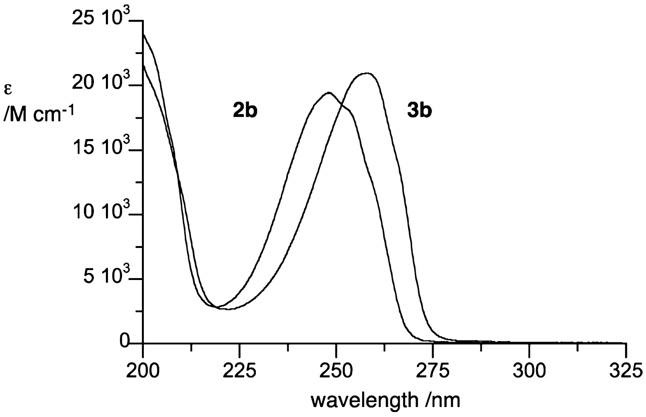

Figure 6. Electronic absorption spectra for **2b** and **3b** (CH_3CN).

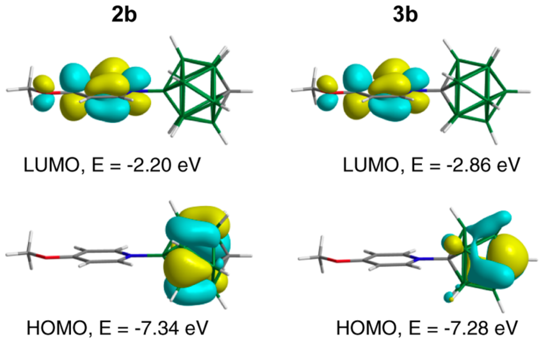

Figure 7. B3LYP/6-31G(d,p)-derived contours and energies of molecular orbitals relevant to low-energy excitations in **2b** and **3b** in vacuum.

X-ray Crystallography. Colorless crystals of **2b** and **3b** were obtained by slow evaporation of CH_2Cl_2/MeOH solutions, and their solid-state structures were determined by low-temperature single-crystal X-ray analysis. Results are shown in Tables 2 and 3 and in Figure 8.

Table 2. Crystallographic Data for 2b and 3b[a]

	2b	3b
empirical formula	$C_7H_{18}B_{11}NO$	$C_7H_{18}B_{11}NO$
fw	251.13	251.13
space group	Pc	$P\bar{1}$
a, Å	7.8904(1)	10.1946(3)
b, Å	10.4796(2)	11.9855(3)
c, Å	17.1104(3)	12.0919(3)
α, deg	90	87.461(2)
β, deg	91.521(2)	77.206(2)
γ, deg	90	77.472(2)
V, Å^3	1414.32(4)	1406.47(7)
Z	4	4
ρ (calcd), g/cm^3	1.179	1.186
μ, mm^{-1}	0.061	0.062
R_{int}	0.0313	0.0341
R[b] ($I > 2\sigma(I)$)	0.0414	0.0464
R_w[c] ($I > 2\sigma(I)$)	0.1076	0.1359
R (all data)	0.0513	0.0574
R_w (all data)	0.1149	0.1483
goodness of fit on F^2	1.061	1.079

[a] Temperature = 100 K, λ = 0.710 73 Å. [b] $R = \sum||F_o| - |F_c||/\sum|F_o|$. [c] $R_w = [\sum[w(F_o^2 - F_c^2)^2]/\sum[w(F_o^2)^2]]^{1/2}$.

B(12)-pyridinium derivative **2b** crystallizes in a Pc monoclinic space group, whereas the C(1)-pyridinium isomer **3b** crystallizes in a $P\bar{1}$ triclinic space group. Both crystal structures contain two molecules in the asymmetric part of the unit cell. In the C(1) isomer **3b**, the C(1)−N bond length is 1.476(1) Å in molecule A and 1.477(1) Å in molecule B, which compares to 1.485 Å calculated at the B3LYP/6-31G(d,p) level of theory. In the B(12) isomer **2b**, the pyridine−{CB_{11}} bonding distance

Table 3. Selected Interatomic Distances and Angles for **2b** and **3b**[a]

	2b	**3b**
N−X	1.547(2) (X = B)	1.476(1) (X = C)
C(1)−B	1.705(5)	1.722(4)
B(2)−B(3)	1.782(2)	1.791(4)
B(2)−B(7)	1.775(3)	1.773(4)
B(7)−B(8)	1.795(4)	1.786(4)
B(12)−B	1.773(7)	1.785(3)
C(1)···B(12)	3.186(4)	3.243(6)
B−B(12)−Y	120.5(1) (Y = N)	121.7(1) (Y = H)
B−C(1)−Y	117.2(2) (Y = H)	118(1) (Y = N)

[a] Average values were calculated for both unique molecules in the unit cell.

is longer: 1.548(2) Å and 1.545(2) Å in the two unique molecules (calculated 1.561 Å). In both isomers, the pyridine ring nearly eclipses the B−H bond; the ring−{1-CB_{11}} torsional angle is 11.8° and 11.3° (calcd 7.4°) in **3b**, and 3.6° and 12.9° (calcd 9.1°) in **2b**.

Analysis of data in Table 3 indicates that the position of the pyridine ring in the cluster has small but noticeable effect on the {1-CB_{11}} cluster geometry. Thus, substitution of the pyridine ring at the B(12) position lowers the Y−B(12)−B angle from 121.7(1)° in **3b** (Y = H) to 120.5(1)° in **2b** (Y = N). On the other hand, the Y−C(1)−B angle slightly expands upon substitution with the pyridine fragment from 117.2(2)° in **2b** (Y = H) to 118(1)° in **3b** (Y = H). Consequently, the C(1)···B(12) distance is shorter for **2b** (3.186(4) Å) than it is in the C(1) isomer **3b** (3.243(6) Å).

Mechanistic Considerations. The transformation of amine **4** to pyridinium derivative **2** is a multistep process, similar to that reported[14] earlier for [*closo*-1-CB_9H_8-1-COOH-6-NH_3]. The proposed mechanism involves the formation of 12-dinitrogen zwitterion **14**, heterolysis of the B−N bond with loss of N_2, trapping of the resulting 12-boronium ylide **15** with a nucleophile, such as 4-methoxypyridine, and formation of **2** (Figure 9).

Previous MP2/6-31+G(d,p)//MP2/6-31G(d,p) level calculations in 50% aqueous EtOH dielectric medium demonstrated[12,14] that the 12-ammonium group in the parent [*closo*-1-$CB_{11}H_{11}$-12-NH_3] (**4b[H]**) is more acidic than the 10-ammonium group in [*closo*-1-CB_9H_9-10-NH_3], whose carboxylic acid derivative [*closo*-1-CB_9H_8-1-COOH-10-NH_3] has been diazotized successfully in pyridine solutions giving an isolable stable dinitrogen acid [*closo*-1-CB_9H_8-1-COOH-10-N_2].[12] This suggests that amine **4b[H]** can also undergo partial deprotonation in pyridine solutions to the extent sufficient for effective diazotization and formation of transient dinitrogen derivative **14b**.

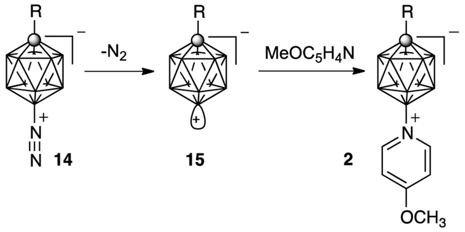

Figure 9. Proposed mechanism for the formation of **2**.

In agreement with experimental observations, DFT computational analysis indicates that dinitrogen [*closo*-1-$CB_{11}H_{11}$-12-N_2] (**14b**) is unstable against loss of N_2 (Table 4). The formation of the ylide **15b** is only +24.8 kcal mol^{-1} endothermic (ΔG_{298} = +14.1 kcal mol^{-1}), which is similar to that calculated for [*closo*-1-CB_9H_8-1-COO-6-N_2]$^-$ in pyridine solutions (24.1 kcal mol^{-1}) and 11.3 kcal mol^{-1} lower than that obtained for [*closo*-1-CB_9H_8-1-COO-10-N_2]$^-$ at the same level of theory in pyridine dielectric medium. This difference is apparently sufficiently large to render [*closo*-1-CB_9H_8-1-COOH-10-N_2] an isolable stable compound,[12] while the two other dinitrogen compounds (including **14b**) exist only as transient species.[14] The subsequent reaction of ylide **15b** with 4-methoxypyridine is strongly exothermic (ΔH = −68.6 kcal mol^{-1}), which is typical for boronium ylides of the 10-vertex analogues.[12]

Table 4. Thermodynamic Parameters (kcal mol^{-1}) for Transformation of **14** to **2**[a]

	14→15	15→2
R	ΔH (ΔG_{298})	ΔH (ΔG_{298})
a COOH	26.0 (15.3)	−70.9 (−58.5)
b H	24.8 (14.1)	−68.6 (−56.7)
d COO^-	24.5 (13.6)	−65.1 (−51.8)
e C_2H_5	25.8 (14.7)	−69.0 (−56.2)

[a] In pyridine dielectric medium (B3LYP/6-31G(d,p) with PCM model). For structures see Figure 9.

Further DFT calculations indicate that the stability of the dinitrogen species **14** depends on the nature of the antipodal

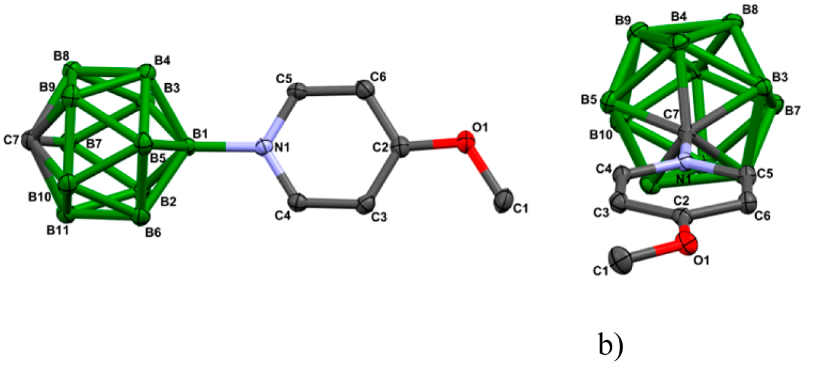

Figure 8. Thermal ellipsoid diagram of (a) 12-(4-methoxypyridinium)-1-carbadodecaborate (**2b**) and (b) 1-(4-methoxypyridinium)-1-carbadodecaborate (**3b**). Hydrogen atoms are omitted for clarity. Pertinent molecular dimensions are listed in Table 3.

substituent. Interestingly, substitution of the C(1) position with a COO$^-$ group, present during diazotization of the amino acid **4a**[**H**] in pyridine solutions, moderately increases propensity of **14d** to loss of N_2, presumably due to electrostatic reasons. In contrast, a moderately electron-donating alkyl group, such as ethyl, and electron-withdrawing COOH stabilize the dinitrogen species **14e** and **14a**, respectively, by ~1 kcal mol^{-1} relative to the parent **14b**.

Interestingly, ^{11}B NMR analysis of the crude reaction mixture taken during the conversion of amine **4c** to pyridinium **2c** and diluted with CD_3CN revealed the presence of a single species, presumably the transient 12-dinitrogen derivative [*closo*-1-$CB_{11}H_{10}$-1-C_5H_{11}-12-N_2] (**14c**), with the characteristic signal at δ −9.3 ppm (Figure 10). At −40 °C, the signal was slowly converting to the signal at +3.6 ppm, characteristic for the expected **2c**, and the process was much faster at ambient temperature. Monitoring of the originally taken NMR sample revealed that the signal related to **2c** and a new signal at +0.2 ppm were evolving at the expense of the signal at −9.3 ppm (Figure 10). This new signal at +0.2 ppm was attributed to [*closo*-1-$CB_{11}H_{10}$-1-C_5H_{11}-12-$NCCD_3$] (**16c**), an adduct of ylide **15c** to acetonitrile-d_3, which upon treatment with H_2O gave the acetamide derivative **17c** with the B(12) signal shifted to −1.8 ppm (Scheme 5). This structural assignment is supported by high-resolution mass spectrometry (HRMS) analysis of the hydrolyzed NMR sample. Similar adducts were observed in thermolysis of dinitrogen derivatives of [*closo*-1-CB_9H_8-1-COOMe-10-N_2],[12] [*closo*-1-CB_9H_9-1-N_2],[11] and [*closo*-$B_{10}H_8$-1,10-$(N_2)_2$][19] in organic nitriles. If correct, derivative **14c** would represent the first experimentally observed dinitrogen derivative of 12-vertex *closo*-borates.

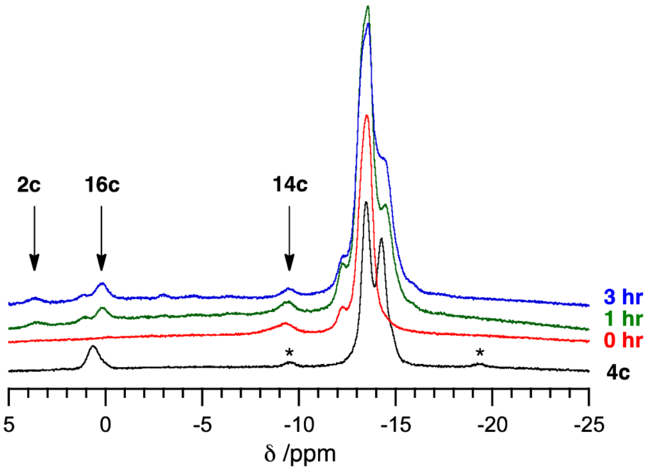

Figure 10. A sequence of ^{11}B NMR spectra showing the transformation of amine **4c**[**NMe$_4$**] (black line) to CD_3CN adduct **16c**. The asterisks indicate trace impurities in the amine. The sample was taken at −40 °C, dissolved in CD_3CN at −40 °C, and placed in the spectrometer at ambient temperature before immediate recording of the spectra.

Scheme 5. Formation of 17c[a]

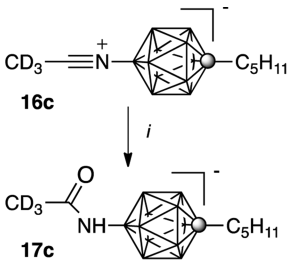

[a]Reagents and conditions: (*i*) H_2O.

The origin for this propensity toward loss of molecular nitrogen (dediazoniation) by some dinitrogen zwitterions lays in the nature of the N−B bond, which is best analyzed for the parent derivatives at the MP2 level of theory. Thus, computational analysis of [*closo*-1-$CB_{11}H_{11}$-12-N_2] (**14b**) in MeCN dielectric medium revealed that the bonding situation of **14b** is similar to that found for [*closo*-1-CB_9H_9-6-N_2] (**18**), and significantly different from the presumably much more stable [*closo*-1-CB_9H_9-10-N_2] (**19**, Table 5).[14] In compounds **14b** and **18** the B−N bond is long (d_{BN} = 1.507 and 1.491 Å, respectively) with low bond order (WBI = 0.74 and 0.76), while the N−N bond is short (d_{NN} = 1.133 and 1.136 Å) with high bond order (WBI = 2.54 and 2.50). This weak bonding in **14b** and **18** is related to the small negative charge (q_B = −0.05 and −0.08) at the B(12) and B(6) atom, respectively. Consequently, both compounds have predicted low thermodynamic stability against loss of N_2 (ΔH = 30.5 and 28.8 kcal/mol, respectively), which renders them unstable at ambient temperature. In contrast, the bonding situation in **19** is significantly better: the B(10)−N bond is markedly shorter (d_{BN} = 1.459 Å), has higher electron density (WBI = 0.80), and the B(10) atom has higher negative charge (q_B = −0.13). This results in increased thermodynamic stability of the species with the highest enthalpy for dediazoniation, (ΔH = 41.8 kcal/mol) among the three zwitterions (Table 5).

Table 5. Bonding Properties of Selected Dinitrogen Derivatives[a]

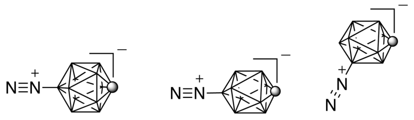

	14b	19[b]	18[b]
$d_{\mathrm{B-N}}$/Å	1.507	1.459	1.491
$d_{\mathrm{N-N}}$/Å	1.133	1.138	1.136
$\mathrm{WBI}_{\mathrm{B-N}}$	0.74	0.80	0.76
$\mathrm{WBI}_{\mathrm{N-N}}$	2.54	2.47	2.50
B[c]	$sp^{6.5}$	$sp^{6.0}$	$sp^{6.0}$
N[c]	$sp^{0.64}$	$sp^{0.65}$	$sp^{0.65}$
q_B	−0.05	−0.13	−0.08
q_N	+0.15	+0.14	+0.13
ΔH/kcal/mol[d]	30.5	41.8	28.8

[a]NBO analysis of the MP2/6-31G(d,p) wave function in MeCN dielectric medium (IPCM model): *d*—distance, WBI—Wiberg bond index, *q*—charge, ΔH—energy of dediazoniation. [b]Partial data from ref 14. [c]Hybridization of the orbital forming the B−N bond. [d]Heterolytic cleavage of the B−N bond.

■ SUMMARY AND CONCLUSIONS

We have developed a method for the efficient preparation of B(12)-substituted pyridinium zwitterions derived from the [*closo*-1-$CB_{11}H_{12}$]$^-$ anion (**B**). This new method represents an approximately 3-fold improvement in yield over the previously employed methodology. The improved process involves synthesis of a 4-methoxypyridinium zwitterion followed by demethylation and realkylation with an alkyl triflate. The method was demonstrated for the heptyl substituent, although more complex alkyl groups, such as *trans*-4-pentylcyclohexylmethyl, should work equally well, opening up convenient access to a potentially broad class of polar materials. Overall, polar pyridinium derivatives, such as **1**, are available in eight steps and ~12% yield from commercial $B_{10}H_{14}$.

A comparison of the two 4-methoxypyridinium isomers, **2b** and **3b**, demonstrated that they generally have similar spectroscopic properties and molecular structures. Detailed analysis revealed that the pyridine ring in **3b** is more deshielded, **3b** has lower cage-to-pyridine excitation energy and 50% higher molecular dipole moment. The latter causes these C(1) zwitterions (e.g., **3** and **13**) to be more crystalline (higher melting), while the isomeric derivatives **1**, such as **1c**, have lower melting points, and some exhibit liquid crystalline behavior.

We also computationally assessed the reaction mechanism for the formation of the B(12)-substituted pyridinium derivatives of [*closo*-1-$CB_{11}H_{12}$]$^-$ anion. The calculations confirmed that dinitrogen derivatives of the [*closo*-1-$CB_{11}H_{12}$]$^-$ anion are generally unstable and are therefore difficult to isolate. Nonetheless, ^{11}B NMR evidence for the existence of the dinitrogen derivative **14c** as a transient species was presented.

The findings reported here represent further development and understanding of the fundamental chemistry of the [*closo*-1-$CB_{11}H_{12}$]$^-$ anion and contribute to our ongoing program in designing liquid crystalline materials incorporating boron clusters.

COMPUTATIONAL DETAILS

Quantum-mechanical calculations were carried out using Gaussian 09 suite of programs.[20] Geometry optimizations for unconstrained conformers of **1c** and **13** with the most extended molecular shapes were undertaken at the B3LYP/6-31G(d,p) level of theory using default convergence limits. The alkyl groups were set in all-trans conformation in the input structure.

Calculations involving reactive intermediates were carried out with the B3LYP and MP2(fc) methods with 6-31G(d,p) basis set. Geometry optimizations were undertaken using appropriate symmetry constraints and tight convergence limits. Vibrational frequencies were used to characterize the nature of the stationary points and to obtain thermodynamic parameters. Zero-point energy (ZPE) corrections were scaled by 0.9806.[21] Hybridization parameters, Wiberg Bond Index (WBI) matrix, and natural charges were obtained using the NBO algorithm supplied in the Gaussian 09 package. Population analysis of the MP2 wave function (MP2//MP2) was performed using the DENSITY(MP2) keyword. The IPCM solvation model[22] was used with default parameters and $\varepsilon = 36.64$ for MeCN. The PCM model[23] was implemented using the SCRF (solvent = pyridine) keyword.

EXPERIMENTAL SECTION

General. Reagents and solvents were obtained commercially. Reactions were carried out under Ar, and subsequent manipulations were conducted in air. NMR spectra were obtained at 128 MHz (^{11}B) and 400 MHz (^{1}H) in CD_3CN or $CDCl_3$. ^{1}H NMR spectra were referenced to the solvent, and ^{11}B NMR chemical shifts were referenced to an external boric acid sample in CH_3OH (18.1 ppm). Optical microscopy and phase identification were performed using a polarized microscope equipped with a hot stage. Thermal analysis was obtained using a TA Instruments DSC using small samples of ~0.5–1.0 mg. Transition temperatures (onset) and enthalpies were obtained on heating using small samples (0.5–1 mg) and a heating rate of 5 K min^{-1} under a flow of nitrogen gas unless specified otherwise.

X-ray Data Collection. Single-crystal X-ray measurement for **2b** was performed with a Supernova Dual diffractometer equipped with an Atlas detector, whereas for **3b** it was performed with a SuperNova diffractometer equipped with an Eos detector. Both measurements were conducted at 100 K using the Mo Kα radiation. The crystals were positioned at ~50 mm from the CCD detectors. A total number of 501 frames were collected at 1° intervals with a counting time of 25 s for **2b**, whereas 1328 frames were collected for **3b** with a counting time of 15 s. The data were corrected for Lorentzian and polarization effects. Data reduction and analyses were carried out with the Crysalis program.[24] Both structures were solved by direct methods using SHELXS-97 and refined using SHELXL-97[25] within the Olex2 program.[26] The refinement was based on F^2 for all reflections except those with very negative F^2. Weighted R factors (wR) and all goodness-of-fit (GOF) values are based on F^2. Conventional R factors are based on F with F set to zero for negative F^2. The $F_o^2 > 2\sigma(F_o^2)$ criterion was used only for calculating the R factors, and it is not relevant to the choice of reflections for the refinement. The R factors based on F^2 are about twice as large as those based on F. Scattering factors were taken from the International Tables for Crystallography.[27] All hydrogen atoms were placed in idealized geometrical positions. Additional crystallographic data are available in the Supporting Information.

12-(4-Heptyloxypyridinium)-1-carbadodecaborate (1b). *Method A.* Pure [*closo*-1-$CB_{11}H_{11}$-12-NH_2]$^-$[NMe_4]$^+$ (**4b[NMe$_4$]**, 100 mg, 0.63 mmol) was dissolved in freshly distilled 4-heptyloxypyridine (4 mL), and the solution was cooled to −20 °C. Solid [NO]$^+$[PF_6]$^-$ (0.66 g, 3.77 mmol) was added in four portions in 10 min intervals to the vigorously stirred mixture. The reaction mixture was allowed to warm to room temperature (rt) and stirred for 2 h. The brown suspension was washed with hexane (5 × 10 mL) and then dissolved in 10% HCl (30 mL). The aqueous layer was extracted with Et_2O (4 × 10 mL), the organic layer was dried (Na_2SO_4), and solvents were evaporated. The crude product was purified by column chromatography (SiO_2, CH_2Cl_2/hexane, 1:2) to give 31 mg (15% yield) of pure **1b**, which was recrystallized from isooctane (2×) giving a white crystalline solid: mp 99 °C; ^{1}H NMR (400 MHz, CD_3CN) δ 0.90 (t, J = 6.8 Hz, 3H), 1.0–2.5 (br m, 10H), 1.25–1.49 (m, 8H), 1.81 (quint, J = 7.0 Hz, 2H), 2.59 (br s, 1H), 4.23 (t, J = 6.6 Hz, 2H), 7.14 (d, J = 7.5 Hz, 2H), 8.43 (d, J = 7.2 Hz, 2H); ^{13}C NMR (125.8 MHz, CD_3CN) δ 14.7, 23.6, 26.3, 29.4, 29.9, 32.8, 47.2 (br), 71.9, 113.8, 148.2; ^{11}B NMR (128 MHz, CD_3CN) δ −16.5 (d, J = 158 Hz, 5B), −13.6 (d, J = 140 Hz, 5B), 4.8 (s, 1B). Anal. Calcd for $C_{13}H_{30}B_{11}NO$: C, 46.57; H, 9.02; N, 4.18. Found: C, 46.56; H, 9.21; N, 4.18%.

Method B. Pyridone **5b[NMe$_4$]** (35 mg, 0.11 mmol) was dissolved in CH_2Cl_2 (1 mL), and heptyl triflate[5] (28 mg, 0.11 mmol) was added dropwise while stirring. Reaction progress was monitored by thin-layer chromatography (TLC) (CH_2Cl_2). After 1 h the organic layer was passed through a short silica gel plug (CH_2Cl_2), the solvents were removed, and the residue was washed with cold pentane to give 30 mg (80% yield) of **1b** as colorless crystals.

12-(4-Heptyloxypyridinium)-1-pentyl-1-carbadodecaborate (1c). Pyridone **5c[NMe$_4$]** (30 mg, 0.08 mmol) was dissolved in CH_2Cl_2 (1 mL), and heptyl triflate[5] (28 mg, 0.09 mmol) in CH_2Cl_2 (0.5 mL) was added dropwise, while stirring. Reaction progress was monitored by TLC (CH_2Cl_2). After 2 h the reaction mixture was passed through a short silica gel plug (CH_2Cl_2). Solvents were removed giving 32 mg (100% yield) of crude **1c** as a white solid, which was recrystallized twice from isooctane: ^{1}H NMR (400 MHz, CD_3CN) δ 0.86 (t, J = 7.2 Hz, 3H), 0.90 (t, J = 6.9 Hz, 3H), 1.0–2.5 (br m, 10H), 1.10–1.20 (m, 2H), 1.21–1.48 (m, 12H), 1.75–1.82 (m, 2H), 1.85 (br t, J = 8.5 Hz, 2H), 4.22 (t, J = 6.6 Hz, 2H), 7.12 (d, J = 7.5 Hz, 2H), 8.41 (d, J = 7.4 Hz, 2H); ^{11}B NMR (128 MHz, CD_3CN) δ −13.7 (d, J = 146 Hz, 10B), 3.6 (s, 1B). Anal. Calcd for $C_{18}H_{40}B_{11}NO$: C, 53.33; H, 9.94; N, 3.45. Found: C, 53.45; H, 9.87; N, 3.52%.

12-(4-Methoxypyridinium)-1-carbadodecaborate (2b). Amine [*closo*-1-$CB_{11}H_{11}$-12-NH_2]$^-$[NMe_4]$^+$ (**4b[NMe$_4$]**, 290 mg, 1.25 mmol) containing ~22% of the 7-isomer **8b[NMe$_4$]** was dissolved in freshly distilled 4-methoxypyridine (8 mL), and the solution was cooled to −20 °C. Solid $[NO]^+[PF_6]^-$ (1.32 g, 7.56 mmol) was added in six portions in 10 min intervals, with vigorous mechanical stirring. After each addition, the solution turned green. The reaction was warmed to rt and stirred for 2 h. The brown suspension was washed with hexane (5 × 10 mL) and then dissolved in 10% HCl (50 mL). The aqueous layer was extracted with Et_2O (4 × 10 mL), the organic layer was dried (Na_2SO_4), and solvents were evaporated giving 377 mg of crude material. Separation by column chromatography (SiO_2, CH_2Cl_2/hexane, 3:2) gave 130 mg (53% yield based on pure **4b**[**NMe$_4$**]) of pure **2b** (R_f = 0.61), which was recrystallized twice from isooctane/toluene giving colorless needles: mp 221 °C; ^1H NMR (400 MHz, CD_3CN) δ 1.0−2.5 (br m, 10H), 2.60 (br s, 1H), 4.01 (s, 3H), 7.18 (d, J = 7.5 Hz, 2H), 8.47 (d, J = 6.8 Hz, 2H); ^{13}C NMR (125.8 MHz, CD_3CN) δ 47.1 (br), 58.4, 113.5, 148.3, 171.8; ^{11}B NMR (128 MHz, CD_3CN) δ −16.5 (d, J = 156 Hz, 5B), −13.6 (d, J = 141 Hz, 5B), 4.8 (s, 1B). Anal. Calcd for $C_7H_{18}B_{11}NO$: C, 33.48; H, 7.22; N, 5.58. Found: C, 33.70; H, 7.29; N, 5.62%.

The more polar fraction contained the 7-(4-methoxypyridinium) isomer **9b** (SiO_2, CH_2Cl_2/hexane, 3:2, R_f = 0.46): ^1H NMR (400 MHz, CD_3CN) δ 1.0−2.5 (br m, 10H), 2.72 (br s, 1H), 4.05 (s, 3H), 7.24 (d, J = 7.5 Hz, 2H), 8.64 (d, J = 6.8 Hz, 2H); ^{11}B NMR (128 MHz, CD_3CN) δ −18.6 (d, J = 141 Hz, 1B), −16.4 (d, J = 155 Hz, 4B), −13.6 (d, J = 130 Hz, 4B), −6.7 (d, J = 138 Hz, 1B), 0.6 (s, 1B); HRMS, calcd for [M−Me+H] $C_6H_{15}B_{11}NO$: m/z = 238.2184; found: m/z = 238.2213.

12-(4-Methoxypyridinium)-1-pentyl-1-carbadodecaborate (2c). Following the procedure for preparation of **2b**, amine $[closo\text{-}1\text{-}CB_{11}H_{10}\text{-}12\text{-}NH_2\text{-}1\text{-}C_5H_{11}]^-[NMe_4]^+$ (**4c**[**NMe$_4$**], 250 mg, 0.83 mmol, 23% of the 7-isomer **8c**[**NMe$_4$**]) in 4-methoxypyridine (5 mL) was treated with $[NO]^+[PF_6]^-$ (0.87 g, 4.97 mmol). The resulting brown crude product was separated by column chromatography (SiO_2, CH_2Cl_2/hexane, 1:1) giving 87 mg (45% yield based on pure **4c**[**NMe$_4$**]) of **2c**. Recrystallization from isooctane/toluene (2×) gave **2c** as colorless needles: mp 165 °C; ^1H NMR (400 MHz, CD_3CN) δ 0.86 (t, J = 7.2 Hz, 3H), 1.0−2.5 (br m, 10H), 1.10−1.20 (m, 2H), 1.21−1.35 (m, 4H), 1.85 (br t, J = 8.5 Hz, 2H), 4.0 (s, 3H), 7.16 (d, J = 7.5 Hz, 2H), 8.44 (d, J = 7.3 Hz, 2H); ^{11}B NMR (128 MHz, CD_3CN) δ −13.7 (d, J = 146 Hz, 10B), 3.6 (s, 1B). Anal. Calcd for $C_{12}H_{28}B_{11}NO$: C, 44.86; H, 8.79; N, 4.36. Found: C, 45.13; H, 8.90; N, 4.38%.

Further elution of the column gave the 7-isomer **9c**: ^1H NMR (400 MHz, CD_3CN) δ 0.87 (t, J = 7.2 Hz, 3H), 1.0−2.5 (br m, 10H), 1.10−1.20 (m, 2H), 1.21−1.35 (m, 4H), 1.88 (br t, J = 8.6 Hz, 2H), 4.0 (s, 3H), 7.23 (d, J = 7.5 Hz, 2H), 8.63 (d, J = 7.1 Hz, 2H); ^{11}B NMR (128 MHz, CD_3CN) δ −15.6 (d, 1B), −13.4 (d, J = 126 Hz, 8B), −9.67 (d, J = 140 Hz, 1B), 0.64 (s, 1B); HRMS, calcd for [M−Me+H] $C_{11}H_{26}B_{11}NO$: m/z = 309.3045; found: m/z = 309.3027.

1-(4-Methoxypyridinium)-1-carbadodecaborate (3b). Amine **12**[**NMe$_4$**] (200 mg, 0.86 mmol) was dissolved in THF (3 mL), and crude 4-methoxypyrylium salt (**11**, 269 mg, 1.0 mmol, prepared by methylation of 4*H*-pyran-4-one with CF_3SO_3Me in THF according to a general procedure[5]) in THF (1 mL) was added. The reaction mixture was stirred overnight at rt, solvents were removed, and the brown residue was purified by column chromatography (SiO_2, CH_2Cl_2) to give the 35 mg (16% yield) of **3b**. The product was washed with hot toluene and then recrystallized twice from CH_3OH containing few drops of CH_3CN: mp > 260 °C; ^1H NMR (400 MHz, CD_3CN) δ 1.0−2.9 (br m, 10H), 4.10 (s, 3H), 7.24 (d, J = 7.8 Hz, 2H), 8.83 (d, J = 7.8 Hz, 2H); ^{13}C NMR (125.8 MHz, CD_3CN) δ 59.4, 84.8 (br), 114.1, 146.2, 173.4; ^{11}B NMR (128 MHz, CD_3CN) δ −13.7 (d, J = 130 Hz, 5B), −12.9 (d, J = 126 Hz, 5B), −8.1 (d, J = 137 Hz, 1B). Anal. Calcd for $C_7H_{18}B_{11}NO$: C, 33.48; H, 6.90; N, 5.58. Found: C, 33.90; H, 6.90; N, 5.68%.

$[closo\text{-}1\text{-}CB_{11}H_{11}\text{-}12\text{-}NH_2]^-[NMe_4]^+$ (4b[NMe$_4$]).[17] $[closo\text{-}1\text{-}CB_{11}H_{11}\text{-}12\text{-}I]^-[Cs]^+$ (**6b**[**Cs**],[18] 670 mg, 1.67 mmol) containing 23% of the 7 isomer **7b**[**Cs**] was added to a solution of lithium hexamethyldisilazane (LiHMDS, 35 mL, 35 mmol, 1.0 M in THF) at rt under N_2. The light-orange suspension was then stirred for 15 min. Pd_2dba_3 (91 mg, 0.1 mmol) and 2-(dicyclohexylphosphino)biphenyl (41 mg, 0.40 mmol) were quickly added, and the reaction mixture was stirred at reflux for 16 h. After cooling to 0 °C, 20% HCl (80 mL) was added slowly to quench unreacted LiHMDS. THF was removed in vacuo giving a dark orange liquid, which was extracted with Et_2O (3 × 50 mL). The organic extracts were dried (Na_2SO_4), and solvents were removed. The resulting brown residue was redissolved in Et_2O, H_2O was added (10 mL), and the Et_2O was removed in vacuo. The aqueous layer was filtered, and the process was repeated four more times to remove phosphonium byproducts. The aqueous layers were combined, and $[NEt_4]^+Br^-$ (350 mg, 1.67 mmol) was added resulting in a white precipitation. The suspension was filtered through Celite; the filtrate was acidified with concentrated HCl (5 mL) and extracted with Et_2O (3 × 50 mL). The organic layers were combined and dried (Na_2SO_4), and the solvents were evaporated giving 90 mg (40% yield) of an off-white solid: $\{^1H\}^{11}B$ NMR (128 MHz, CD_3CN) δ major isomer **4b**[**Cs**] (77%) −16.6 (5B), −13.9 (5B), −0.8 (1B); minor isomer **8b**[**Cs**] (23%) δ −19.0, −12.5, −6.9, −5.4. The solid was treated with an aqueous solution of $[NMe_4]^+[OH]^-\cdot 5H_2O$ (453 mg, 2.50 mmol), and the resulting suspension was extracted into CH_2Cl_2 (3 × 20 mL). The organic layer was dried (Na_2SO_4), and CH_2Cl_2 was removed in vacuo to give a white crystalline solid of **4b**[**NMe$_4$**] containing 23% of the 7-isomer **8b**[**NMe$_4$**]: $\{^1H\}^{11}B$ NMR (128 MHz, CD_3CN) δ major isomer −17.2 (5B), −13.4 (5B), 2.8 (1B); minor isomer δ −22.2, −14.6, −6.5, 0.2.

$[closo\text{-}1\text{-}CB_{11}H_{10}\text{-}1\text{-}C_5H_{11}\text{-}12\text{-}NH_2]^-[\ NMe_4]^+$ (4c[NMe$_4$]). $[closo\text{-}1\text{-}CB_{11}H_{10}\text{-}1\text{-}C_5H_{11}\text{-}12\text{-}I]^-[Cs]^+$ (**6c**[**Cs**], 784 mg, 1.66 mmol) containing 23% of the 7-isomer **7c**[**Cs**] was reacted with lithium hexamethyldisilazane (LiHMDS, 33 mL, 33 mmol, 1.0 M in THF) in the presence of Pd_2dba_3 (91 mg, 0.1 mmol) and 2-(dicyclohexylphosphino)biphenyl (141 mg, 0.40 mmol) as described for the synthesis of the parent **4b**[**NMe$_4$**]. The ethereal extract of the crude product was evaporated giving a brown solid, which was purified by column chromatography (CH_2Cl_2 then 10% CH_3CN in CH_2Cl_2). The solvents were evaporated, and the resulting brown solid was washed with hot hexane giving 370 mg (97% yield) of crude amine **4c**[**H**] contaminated with ∼23% of the 7-isomer **8c**[**H**]: ^1H NMR (400 MHz, CD_3CN) δ major isomer 0.85 (t, J = 7.3 Hz, 3H), 1.0−2.5 (br m, 10H), 1.1−1.2 (m, 2H), 1.21−1.32 (m, 4H), 1.80 (br t, J = 10.7 Hz, 2H); ^{11}B NMR (128 MHz, CD_3CN) δ-13.9 (d, J = 147 Hz, 10B), −2.2 (s, 1B); minor isomer δ −16.1, −10.0, −5.4.

The brown solid was treated with a solution of $[NMe_4]^+OH^-\cdot 5H_2O$, and the resulting precipitation was extracted into CH_2Cl_2. The organic layers were combined and dried (Na_2SO_4), and the solvents were evaporated giving 400 mg (81% yield) of **4c**[**NMe$_4$**] as a tan solid contaminated with the 7-isomer **8c**[**NMe$_4$**].

Major isomer **4c**[**NMe$_4$**]: ^1H NMR (400 MHz, CD_3CN) δ 0.85 (t, J = 7.3 Hz, 3H), 1.0−2.5 (br m, 10H), 1.09−1.18 (m, 2H), 1.20−1.32 (m, 4H), 1.80 (br t, J = 8.5 Hz, 2H), 3.1 (s, 12H); ^{11}B NMR (128 MHz, CD_3CN) δ −14.3 (d, J = 127 Hz, 5B), −13.5 (d, J = 118 Hz, 5B), 0.7 (s, 1B).

Minor isomer **8c**[**NMe$_4$**], characteristic signals: ^1H NMR (400 MHz, CD_3CN) δ 0.86 (t, J = 7.3 Hz, 3H); $\{^1H\}^{11}B$ NMR (128 MHz, CD_3CN) δ −19.2, −9.6.

HRMS, calcd for $C_6H_{23}B_{11}N$: m/z = 228.2927; found: m/z = 228.2959.

12-(4-Pyridon-1-yl)-1-carbadodecaborate [NMe$_4$]$^+$ salt (5b-[NMe$_4$]). $[closo\text{-}1\text{-}CB_{11}H_{11}\text{-}12\text{-}(4\text{-}CH_3OC_5H_4N)]$ (**2b**, 100 mg, 0.40 mmol) was dissolved in dry DMF (5 mL), LiCl (50 mg, 1.2 mmol) was added, and the resulting mixture was stirred at 80 °C for 16 h. The reaction mixture was cooled to rt, DMF was removed in vacuo, water (5 mL) containing $[NMe_4]^+Cl^-$ (130 mg, 1.2 mmol) and CH_2Cl_2 (5 mL) was added, and the resulting biphasic system was stirred for 2 h. The organic layer was separated and dried (Na_2SO_4), and the solvents were removed. The oily yellow residue was washed with Et_2O (3 × 5 mL) and dried to give 122 mg (99% yield) of **5b**[**NMe$_4$**] as a white crystalline solid, which was recrystallized twice from a toluene/CH_3CN mixture: mp 251 °C; ^1H NMR (400 MHz, CD_3CN) δ 1.0−2.5 (br m, 10H), 2.43 (br s, 1H) 3.10 (s, 12H), 6.10 (d, J = 7.5 Hz, 2H), 7.61 (d, J = 6.7 Hz, 2H); ^{13}C NMR (125.8 MHz, CD_3CN) δ 45.6 (br), 56.2 (t, J = 8.5 Hz), 117.1, 144.9, 178.0; ^{11}B NMR (128 MHz, CD_3CN) δ −17.0 (d, J = 151 Hz, 5B), −13.7 (d, J = 139 Hz, 5B), 5.4

(s, 1B); HRMS, calcd for $C_6H_{15}B_{11}NO$: m/z = 238.2184; found: m/z = 238.2186. Anal. Calcd for $C_{10}H_{27}B_{11}N_2O$: C, 38.71; H, 8.77; N, 9.03. Found: C, 38.99; H, 8.93; N, 8.96%.

1-Pentyl-12-(4-pyridon-1-yl)-1-carbadodecaborate [NMe$_4$]$^+$ salt (5c[NMe$_4$]). [*closo*-1-$CB_{11}H_{10}$-12-(4-$CH_3OC_5H_4N$)-1-C_5H_{11}] (**2c**, 80 mg, 0.25 mmol) was converted to pyridone **5c**[**NMe$_4$**] using LiCl (32 mg, 0.75 mmol) in DMF (3 mL) as described above for **5b**[**NMe$_4$**]. Double recrystallization from EtOAc/hexane gave pure **5c**[**NMe$_4$**] as colorless crystals: mp 223.5 °C; ^{1}H NMR (400 MHz, CD_3CN) δ 0.86 (t, J = 7.2 Hz, 3H), 1.0−2.5 (br m, 10H), 1.10−1.20 (m, 2H), 1.21−1.37 (m, 4H), 1.85 (br t, J = 8.5 Hz, 2H), 3.1 (s, 12H), 5.95 (d, J = 7.6 Hz, 2H), 7.48 (d, J = 6.3 Hz, 2H); {^{1}H}^{11}B NMR (128 MHz, CD_3CN) δ −13.9 (10B), 4.0 (1B). Anal. Calcd for $C_{15}H_{37}B_{11}N_2O$: C, 47.36; H, 9.80; N, 7.36. Found: C, 47.09; H, 9.96; N, 7.40%.

[*closo*-1-$CB_{11}H_{10}$-1-C_5H_{11}-12-I]$^-$Cs$^+$ (6c[Cs]). Following a modified general procedure,[18] [*closo*-1-$CB_{11}H_{11}$-1-C_5H_{11}]$^-$Cs$^+$ (**10c**[**Cs**], 930 mg, 2.69 mmol) was dissolved in AcOH (15 mL), iodine (682 mg, 2.69 mmol) was added, and the reaction mixture was stirred at 50 °C. Reaction progress was monitored by ^{11}B NMR, and more iodine was added when necessary (to 1.23 g, 4.84 mmol in total). AcOH was removed in vacuo, and the residue was treated with 10% HCl (30 mL) followed by $Na_2S_2O_5$ to reduce the remaining I_2. The resulting yellow aqueous solution was extracted with Et_2O (4 × 30 mL). The organic layers were combined, H_2O (30 mL) was added, and the Et_2O was removed in vacuo. Solid [NEt$_4$]$^+$Br$^-$ (565 mg, 2.69 mmol) was added, and the resulting white precipitation was filtered and dried giving 1.06 g (77% yield) of **6c**[**NEt$_4$**] contaminated with ~22% of the 7-isomer **7c**[**NEt$_4$**]. The product was suspended in 10% HCl (50 mL) and extracted with Et_2O. Water (25 mL) was added to the combined organic layers, and Et_2O was removed in vacuo. The aqueous solution was treated with an excess of CsOH·H_2O to ensure basicity of the solution, and the resulting white precipitation was extracted into Et_2O (5 × 30 mL). The organic layers were combined and dried (Na_2SO_4), and the solvents were evaporated giving 912 mg of mixture of isomers **6c**[**NEt$_4$**] and **7c**[**NEt$_4$**]. Isomerically pure **6c**[**Cs**] was obtained by repeated recrystallization from hot water: mp 225−226 °C; ^{1}H NMR (400 MHz, CD_3CN) δ 0.84 (t, J = 7.3 Hz, 3H), 1.0−2.5 (br m, 10H), 1.15−1.18 (m, 2H), 1.19−1.30 (m, 4H), 1.68 (br t, J = 8.4 Hz, 2H); ^{13}C NMR (125.8 MHz, CD_3CN) δ 14.4, 23.2, 30.9, 32.6, 40.3, 71.7 (br); ^{11}B NMR (128 MHz, CD_3CN) δ −19.0 (s, 1B), −13.0 (d, J = 172 Hz, 5B), −11.6 (d, J = 159 Hz, 5B). Anal. Calcd for $C_6H_{21}B_{11}CsI$: C, 15.27; H, 4.49. Found: C, 15.66; H, 4.50%.

[*closo*-1-$CB_{11}H_{11}$-1-C_5H_{11}]$^-$Cs$^+$ (10c[Cs]). Pure [*closo*-1-$CB_{11}H_{12}$]$^-$Cs$^+$ (1.88 g, 6.81 mmol) was dissolved in freshly distilled THF (100 mL), freshly distilled dry TMEDA (1.0 mL, 6.81 mmol) was added, and the solution was cooled to −78 °C. *n*-BuLi (6.8 mL, 17.0 mmol, 2.5 M in hexanes) was added dropwise to the solution. The reaction mixture was stirred at −78 °C for 15 min and then allowed to warm to rt. The resulting white suspension was stirred for 1.5 h at rt, cooled to 0 °C, and pentyl iodide (4.0 mL, 30.7 mmol) was added slowly. After stirring overnight, water (15 mL) was added to the mixture, and THF was removed in vacuo. The aqueous solution was acidified with concentrated HCl (3 mL) and extracted with Et_2O (3 × 30 mL). Water (20 mL) was added to the ethereal extract, and Et_2O was removed in vacuo. The aqueous solution was treated with an excess of CsOH·H_2O to ensure basicity of the solution, and the resulting white suspension was extracted with Et_2O (5 × 30 mL). The organic layers were combined and dried (Na_2SO_4), and the solvents were evaporated giving 2.22 g (94% yield) of **10c**[**Cs**] as a slightly yellow solid. The crude product (containing ~8% of the starting Cs$^+$ salt by ^{11}B NMR) was recrystallized from hot water (2×) to give 1.98 g (84% yield) of pure **10c**[**Cs**] as a colorless crystalline solid: mp 209 °C; ^{1}H NMR (400 MHz, CD_3CN) δ 0.85 (t, J = 7.3 Hz, 3H), 1.0−2.5 (br m, 10H), 1.1−1.18 (m, 2H), 1.2−1.34 (m, 4H), 1.78 (br t, J = 8.5 Hz, 2H); ^{11}B NMR (128 MHz, CD_3CN) δ −13.2 (d, J = 143 Hz, 10B), −9.9 (d, J = 134 Hz, 1B). Anal. Calcd for $C_6H_{22}B_{11}Cs$: C, 20.82; H, 6.41. Found: C, 21.08; H, 6.67%.

12-(d_3-Acetylamino)-1-pentyl-1-carbadodecaborate (17c). It was formed by decomposition of the putative 12-dinitrogen **14c** in CD_3CN solvent at ambient temperature during 24 h followed by treatment with water and extraction into CH_2Cl_2: ^{11}B NMR (128 MHz, CD_3CN) δ characteristic signal at −1.8; HRMS, calcd for $C_8H_{22}D_2B_{11}NO$: m/z = 271.3080; found: m/z = 271.3087.

■ ASSOCIATED CONTENT

Ⓢ Supporting Information

Additional details on preparation of [*closo*-1-$CB_{11}H_{12}$]$^-$[NEt$_4$]$^+$, details of TD-DFT, archive files for DFT calculations, and crystallographic data in CIF files. This material is available free of charge via the Internet at http://pubs.acs.org. Crystallographic structures have been deposited at CCDC (1025212 and 1025213).

■ AUTHOR INFORMATION

Corresponding Author

*Phone: (615) 322-3458. E-mail: piotr.kaszynski@vanderbilt.edu.

Notes

The authors declare no competing financial interest.

■ ACKNOWLEDGMENTS

This work was supported by the NSF Grant No. DMR-1207585.

■ REFERENCES

(1) Kaszynski, P. In *Boron Science: New Technologies & Applications*; Hosmane, N., Ed.; CRC Press, FL: 2012; pp 305−338.

(2) Kirsch, P.; Bremer, M. *Angew. Chem., Int. Ed.* **2000**, *39*, 4216−4235.

(3) Ringstrand, B.; Kaszynski, P.; Januszko, A.; Young, V. G., Jr. *J. Mater. Chem.* **2009**, *19*, 9204−9212.

(4) Pecyna, J.; Kaszynski, P.; Ringstrand, B.; Bremer, M. *J. Mater. Chem. C* **2014**, *2*, 2956−2964.

(5) Pecyna, J.; Pociecha, D.; Kaszynski, P. *J. Mater. Chem. C* **2014**, *2*, 1585−1519.

(6) Ringstrand, B.; Kaszynski, P. *J. Mater. Chem.* **2010**, *20*, 9613−9615.

(7) Ringstrand, B.; Kaszynski, P. *Acc. Chem. Res.* **2013**, *46*, 214−225.

(8) Körbe, S.; Peter J. Schreiber, P. J.; Michl, J. *Chem. Rev.* **2006**, *106*, 5208−5249.

(9) A recently published optimized procedure provides [*closo*-1-$CB_{11}H_{12}$]$^-$[NEt$_4$]$^+$ in two steps and 66% yield from commercial $B_{10}H_{14}$: Franken, A.; Kennedy, J. D.; Clapper, J.; Sneddon, L. G. *Inorg. Synth.* **2014**, *36*, 180−191.

(10) For more details see the Supporting Information.

(11) Ringstrand, B.; Kaszynski, P.; Franken, A. *Inorg. Chem.* **2009**, *48*, 7313−7329.

(12) Ringstrand, B.; Kaszynski, P.; Young, V. G., Jr.; Janoušek, Z. *Inorg. Chem.* **2010**, *49*, 1166−1179.

(13) Pecyna, J.; Denicola, R. P.; Ringstrand, B.; Jankowiak, A.; Kaszynski, P. *Polyhedron* **2011**, *30*, 2505−2513.

(14) Ringstrand, B.; Kaszynski, P.; Young, V. G., Jr. *Inorg. Chem.* **2011**, *50*, 2654−2660.

(15) Pecyna, J.; Denicola, R. P.; Gray, H. M.; Ringstrand, B.; Kaszynski, P. *Liq. Cryst.* **2014**, *41*, 1188−1198.

(16) Bernard, A. M.; Ghiani, M. R.; Piras, P. P.; Rivoldini, A. *Synthesis* **1989**, 287−289.

(17) Konieczka, S. Z.; Himmelspach, A.; Hailmann, M.; Finze, M. *Eur. J. Inorg. Chem.* **2013**, 134−146.

(18) Valášek, M.; Štursa, J.; Pohl, R.; Michl, J. *Inorg. Chem.* **2010**, *49*, 10255−10263.

(19) Knoth, W. H. *J. Am. Chem. Soc.* **1966**, *88*, 935−939.

(20) Frisch, M. J., Trucks, G. W., Schlegel, H. B., Scuseria, G. E., Robb, M. A., et al. *Gaussian 09,* Revision A.02; Gaussian, Inc.: Wallingford, CT, 2009.

(21) Scott, A. P.; Radom, L. *J. Phys. Chem.* **1996**, *100*, 16502−16513.

(22) Foresman, J. B.; Keith, T. A.; Wiberg, K. B.; Snoonian, J.; Frisch, M. J. *J. Phys. Chem.* **1996**, *100*, 16098−16104.

(23) Cossi, M.; Scalmani, G.; Rega, N.; Barone, V. *J. Chem. Phys.* **2002**, *117*, 43−54 and references therein.

(24) Agilent, *CrysAlis PRO,* Agilent Technologies: Yarnton, England, 2012.

(25) Sheldrick, G. M. *Acta Crystallogr., Sect. A* **2008**, *64*, 112−122.

(26) Dolomanov, O. V.; Bourhis, L. J.; Gildea, R. J.; Howard, J. A. K.; Puschmann, H. *J. Appl. Crystallogr.* **2009**, *42*, 339−341.

(27) *International Tables for Crystallography;* Schmueli, U., Ed.; Springer: New York, 2006.